Waveguide and guided-wave devices consisting of heterostructured photonic crystals

doi: 10.1117/1.1695407

Waveguide and guided-wave devices consisting of heterostructured photonic crystals

Yasuo Ohtera
Hiroyuki Ohkubo
Tohoku University
New Industry Creation Hatchery Center
Japan
E-mail: ohtera@niche.tohoku.ac.jp

Kenta Miura
Japan Science and Technology Agency
Japan

Takashi Sato
Tohoku University
New Industry Creation Hatchery Center
Japan

Takayuki Kawashima
Photonic Lattice Incorporated
Japan

Shirijo Kawakami
Tohoku University
New Industry Creation Hatchery Center
Japan

Abstract. We report a strategy for the industrialization of photonic-crystal-based optical devices, starting with a review of the requirements for passive photonic crystal components. Although they have remarkable properties, such components are difficult to couple to/from optical fibers and have a relatively large propagation loss. We present an approach for meeting the requirements by using heterostructured photonic crystals fabricated by the autocloning technology. A low-loss, simple structured waveguide and sophisticated functional blocks (such as a resonator) can be integrated by a simple process. We first prepare a substrate patterned and corrugated by electron beam lithography and dry etching. Ta_2O_5/SiO_2 multilayers are repeatedly deposited on the substrate, and no other process is needed to complete the chip. After dicing and polishing, the waveguide can be butt-jointed with an optical fiber, and the loss is estimated as 0.1 dB/mm. A resonator with $Q=11{,}700$ is also demonstrated. Recent progress and the future outlooks for the technology are also discussed.
[DOI: 10.1117/1.1695407]

Subject terms: photonic crystal; heterostructure; waveguide; guided-wave device; resonator; Bragg reflector; autocloning; sputter deposition; sputter etching; thermally expanded core fiber.

Paper WDM-12 received Jan. 15, 2004; accepted for publication Feb. 3, 2004.

1 Introduction

1.1 *Pros and Cons*

Recent investigations have revealed that photonic crystal waveguides and guided-wave devices have several advantages as well as some nontrivial problems. The pros are as follows:

1. unique functions such as superprism,[1] resonator,[2] dispersion, etc.
2. small size
3. loss-free bend/corner in the presence of 3-D full photonic bandgap.[3,4]

The cons are as follows:

1. difficulty of coupling to/from external optics (for example, optical fibers)
2. large waveguide loss (4 dB/mm in an excellent experiment[5])
3. difficulty of incorporating low-loss abrupt bends in 2-D slab photonic crystal waveguides[6–8]
4. difficulty of polarization independent operation.

We attempted to overcome some of the cons while keeping the pros by using heterostructured photonic crystals fabricated by our autocloning technology.[9]

1.2 *Requirements for Photonic Crystal Chips*

To enable passive photonic crystal chips to be used in optoelectronic applications, the following scenario should be reasonable. First, they would be coupled from/to optical fibers, and second, the chips would consist of a number of ''functional blocks'' connected by waveguides, and would have a number of input/output ports, each corresponding to a channel.

Our first point is that the tolerable waveguide attenuation is determined by the number of channels. As shown in Fig. 1, the minimum chip size is roughly given by

$$L = 0.2N + 2 \ \ [\mathrm{mm}],$$

where N is the number of channels. In view of this relation, the waveguide attenuation of state of the art photonic crystal waveguides is still too large. As long as a waveguide is used just for wiring, a simple, low-loss waveguide is better than a sophisticated lossy waveguide, while a functional block should take full advantage of magical characteristics of photonic crystals.

Another point is coupling with optical fibers. Butt-jointing is more convenient than lens coupling. Typical op-

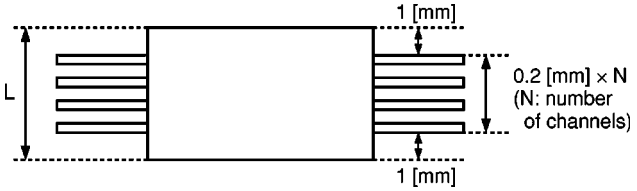

Fig. 1 Relation between the size of an optical chip and the number of channels.

 0091-3286/2004/$15.00

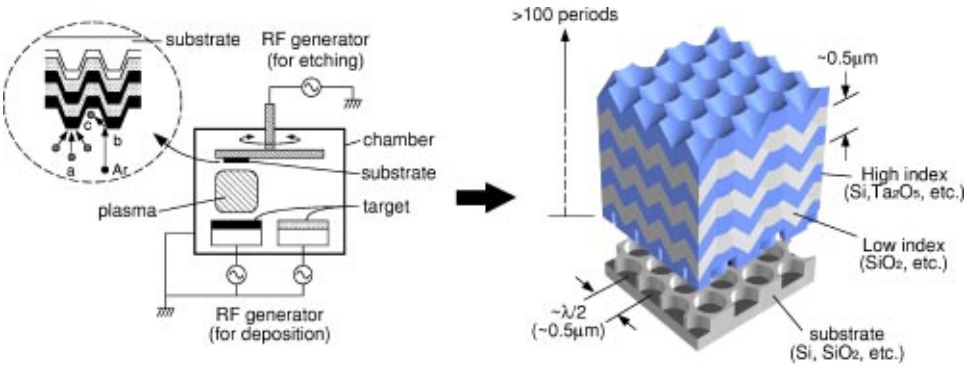

Fig. 2 Principle of the autocloning technology. The inset of the left figure illustrates three elementary processes of the autocloning; i.e., a, deposition by particles coming from a target; b, sputter etching by normally incident ions; and c, redeposition of film materials, respectively.

tical fibers have a mode diameter of 10 μm, and the mode spot size of optical fibers can be reduced to as small as 5 μm (a high-Δ fiber; the doped Germania concentration is very high). Conventional optical fibers and high-Δ fibers can be fusion-spliced and mode-matched by the thermally expanded core (TEC) technique.[10]

Many researchers working on submicrometer-sized waveguides look for ways of tapering the mode spot size. However, tapering in the surface-normal direction is very difficult. This problem can be overcome by using an integrated waveguide that is mode-matched with a high-Δ fiber and integrated with functional photonic crystal functional blocks. This is the strategy of our group.

2 Background

2.1 *Effective Dielectric Constant*

Passbands and stopbands of periodic structures are well known. In a stopband, the wave is proportional to $\exp(-\alpha z)$, whereas in a passband it is proportional to $\exp(-jnz/2\pi)$. In this context, a stopband is characterized by an imaginary value of the refractive index, i.e., a negative value of the dielectric constant.

At the band edge, several unusual characteristics are present such as the superprism effect[1] and strong frequency dependence of the group delay.

2.2 *Autocloning*

Fabrication of 2-D periodic structures is usually not very difficult, but fabrication of structures periodic in the surface-normal direction is a challenge. We have developed a process technology (autocloning) for fabricating a 3-D periodic structure. The technology takes advantage of the evolution of surface shape in sputter-deposition and sputter-etching processes on a corrugated substrate. Under appropriate conditions, the shape of the surface automatically looks for a stationary corrugation. We proceed as follows. As shown in Fig. 2(a), we sputter-deposit (with a small fraction of sputter-etching) two kinds of dielectric materials alternately on a substrate having 2-D periodic corrugations. By virtue of the autocloning effect, we obtain a 3-D periodic structure as shown in Fig. 2(b).

Another advantage of this method is that a heterostructure can be fabricated. Even if the substrate has a number of blocks having different lattice types and/or lattice constants, we can still ''grow'' different crystals simultaneously. As shown in Fig. 3, a heterostructured crystal is successfully grown on a substrate that was patterned by electron beam lithography and dry etching. By utilizing such property, an integrated photonic chip, which consists of waveguide channels and a number of guided-wave functional parts, can be easily fabricated.

3 Waveguide

3.1 *Design and Fabrication*

We decided that the input/output port of our chip should be mode-matched with a high-Δ fiber having the smallest spot size available (roughly 5 μm). Since our waveguide can be designed to have the same mode spot size, a taper section is not required. Schematic view of our channel waveguide is shown in Fig. 4. The waveguide has nine different regions in its cross section. The multilayer consists of Ta_2O_5 ($n=2.1$) and SiO_2 ($n=1.5$). In the horizontal direction, the flat region acts as a core, while the wavy regions act as claddings. The design procedure of this type of waveguide is as follows.

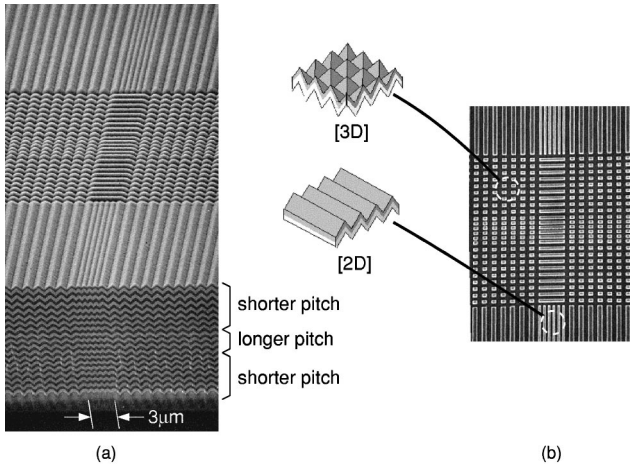

Fig. 3 Fabrication of a heterostructured photonic crystal: (a) SEM photograph of the top surface and the cross section, and (b) patterned substrate (black indicates depression).

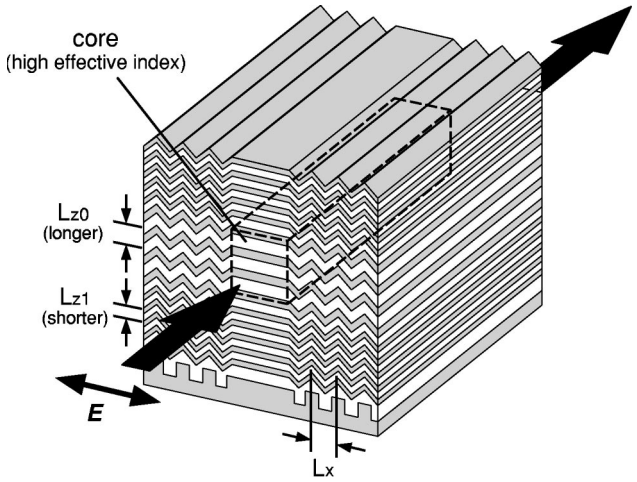

Fig. 4 Schematic view of a flat-core-type channel waveguide.

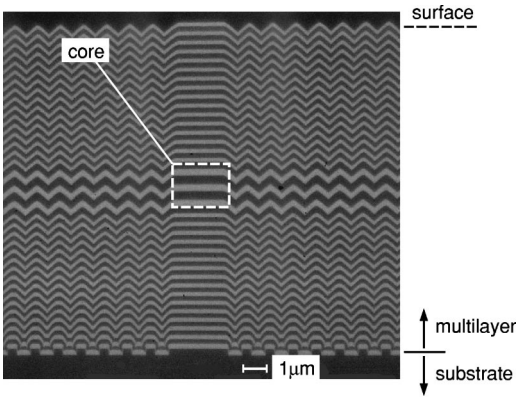

Fig. 6 SEM picture of the cross section of a fabricated channel waveguide. Dark and bright layers correspond to SiO_2 and Ta_2O_5, respectively.

1. We concentrate on the TE polarization (the *E* vector parallel to the plane).
2. Wave confinement in the perpendicular and in-plane directions is done by the difference of effective refractive indexes of each domain of the heterostructure. We make use of the effect that the flat multilayer has a larger effective refractive index than that of wavy multilayers for horizontally polarized light.
3. We choose to make the waveguide uniform (does not have periodicity) in the longitudinal direction, as we prefer waveguides of a simple structure for wiring.
4. The fill factor of Ta_2O_5 is kept common to all heterostructures.

An example of the structural parameters in the waveguide cross section is shown in Fig. 5(b). The relation between the wavelength and effective refractive indexes is calculated by the finite-difference time-domain (FDTD) method. The result and the effective index profile at $\lambda=1550$ nm is shown in Figs. 5(a) and 5(c), respectively. In this design, the effective index differences (Δ) between the core and the cladding in vertical and horizontal directions are approximately 2.3% and 1.9%, respectively.

The fabricated sample after the deposition process is shown in Fig. 6. The cross section shows that the heterointerfaces are parallel or normal to the substrate, but more importantly that the shape of the surface corrugation in the claddings improves as the deposition proceeds. This occurs because the surface shape tends toward the stationary pattern.

3.2 *Characterization*

After deposition of the sample, we diced the chip and polished the ends for optical characterization. We first measured the propagation loss of the waveguide. The waveguide is butt-jointed to a high-D single-mode fiber. The output beam from another end of the waveguide is colli-

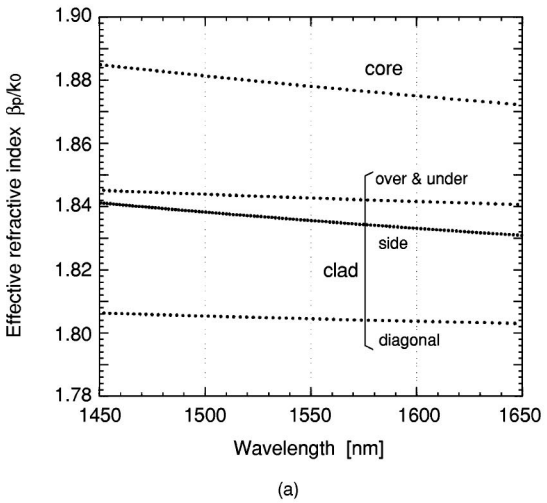

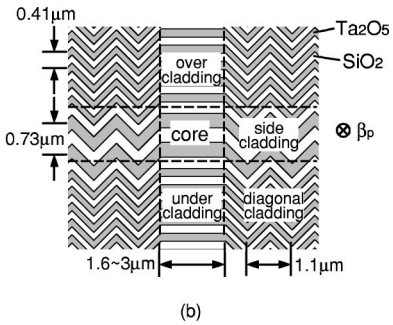

1.805	1.843	1.805
1.836	1.878	1.836
1.805	1.843	1.805

(c)

Fig. 5 Design of the heterostructured channel waveguide: (a) calculated effective refractive index of each crystal region, (b) structural parameters of the heterostructure, and (c) effective refractive index profile at $\lambda=1550$ nm.

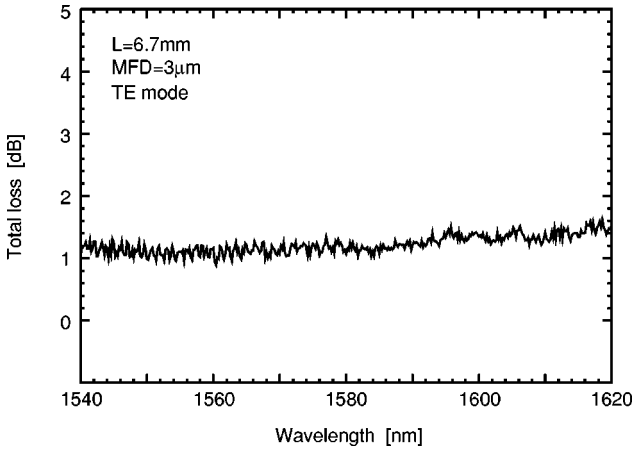

Fig. 7 Measured transmission spectrum of the channel waveguide. Length and the mode field diameter (MFD) are 6.7 mm and 3 μm, respectively. The loss includes coupling loss between the waveguide facet and the fiber at the input port.

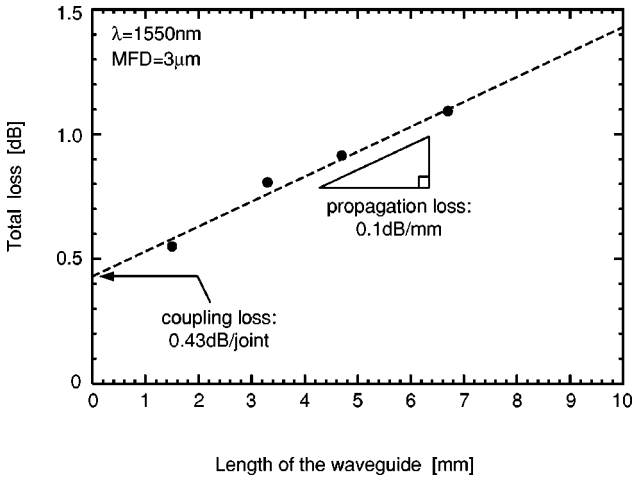

Fig. 8 Result of the loss evaluation at $\lambda=1550$ nm by the cut-back method.

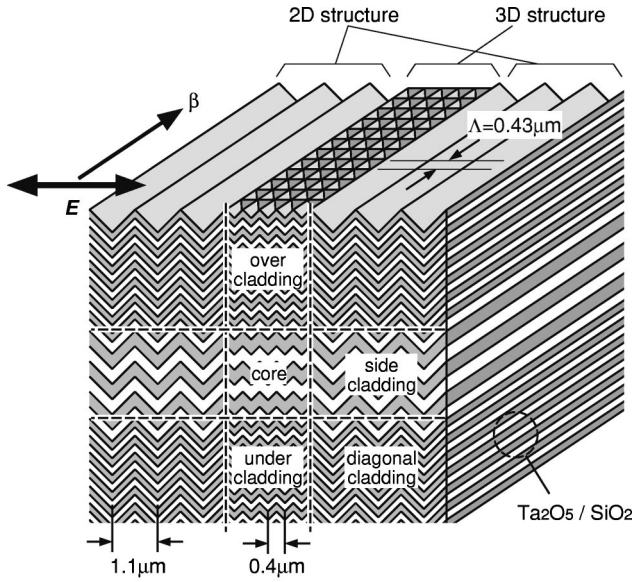

Fig. 9 Schematic view of an inline distributed Bragg reflector (DBR). Core region consists of 3-D autocloning layers.

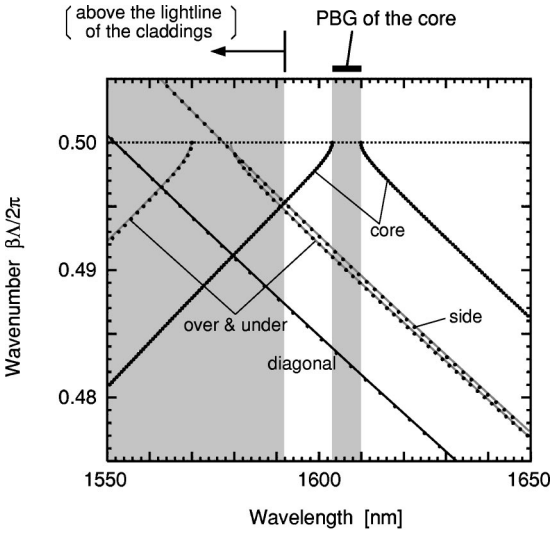

Fig. 10 Calculated dispersion relation of each crystal region of the inline DBR. In the gray region at the left-half of the graph, finite radiation will occur.

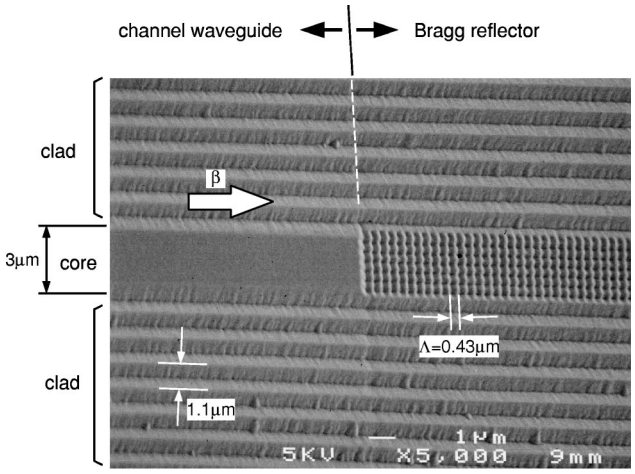

Fig. 11 SEM picture of the surface around the interface between the channel waveguide and the DBR.

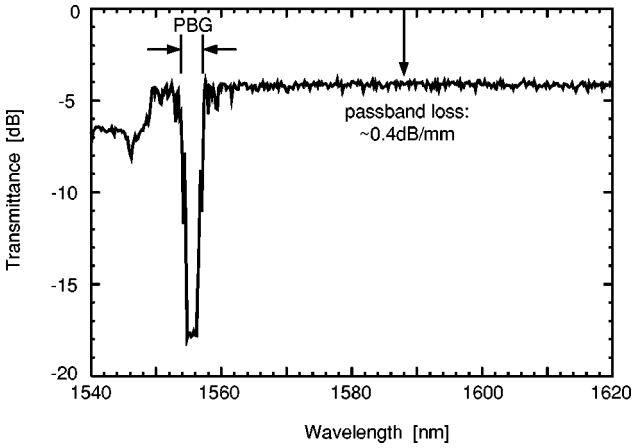

Fig. 12 Measured transmission spectrum of the sample, which consists of 7.5 mm of the channel waveguide and 2.0 mm of the DBR part.

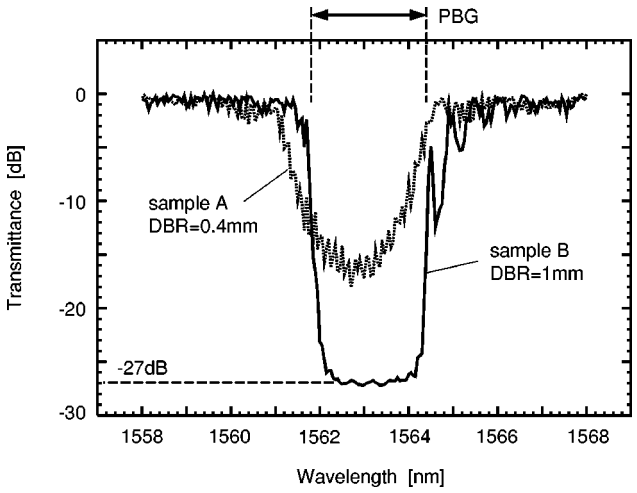

Fig. 13 Magnified view of transmission spectra of other DBR samples. The lengths of the DBR part are 0.4 mm (sample A) and 1.0 mm (sample B), respectively.

mated by a high-NA lens before detection. Figure 7 shows a measured transmission spectrum of a waveguide of length 6.7 mm. The spectrum is almost flat with respect to the wavelength. Next, we tried to evaluate the coupling and propagation losses by the cut-back method. The result is shown in Fig. 8. We estimate that the coupling loss at the waveguide end is approximately 0.43 dB. The net propagation loss is about 0.1 dB/mm, which is low enough for a chip of the order of 1 cm. The small waveguide attenuation is due to the following reasons. 1. The unit cell of the waveguide is uniform in the longitudinal direction, hence multiple reflection/scattering is small. 2. The core consists of a flat multilayer, by which the light scattering at the layer interfaces is minimized. 3. The autocloning process has a self-healing property (see Fig. 6), i.e., small fluctuations in the substrate/lower layers are extinguished during the autocloning process.

4 Functional Block 1: Bragg Reflector

Our strategy is to integrate several functional blocks on a chip and connect them by waveguides. Many different functions are available, and we chose a distributed Bragg reflector (DBR) and a resonator for the first demonstration. In this section, concept, design, and the result of experiments with the DBR are described.

4.1 *Design and Fabrication*

Schematic view of an inline DBR is shown in Fig. 9. The core region of the DBR consists of a 3-D periodic structure. In our previous work,[11] we used a 2-D periodic structure as a DBR and utilized its Γ-point photonic band gap (PBG). Since the operation frequency was placed above the light line, finite out-of-plane radiation occurred at DBRs. On the other hand, in the present 3-D DBR, the first PBG at the Brillouin zone edge opens below the light line. Figure 10 shows calculated dispersion relations of each region of the DBR. The core has a PBG of width ~7 nm centered at $\lambda=1606$ nm. In the right-half of the figure ($\lambda>1592$ nm), the wavenumber (propagation constant) of the core becomes larger than that of the claddings, by which the modal field is confined in the core region even in the PBG wavelength.

The surface view around the waveguide/DBR interface of a fabricated sample is shown in Fig. 11. One can see that three crystal regions with different dimensions (1-D: flat layer; 2-D: claddings; 3-D: DBR part) are successfully formed. Also, the boundary between the flat core region and the DBR is well defined.

4.2 *Characterization*

The characteristics of the sample are evaluated with the same setup as explained in Sec. 3.3. The measured transmission spectrum is shown in Fig. 12. In accordance with the dispersion relation, a PBG of the width of a few nanometers appeared near the short-wavelength edge of the broad and low-loss passband. The measured transmission loss at the long-wavelength side passband is of the order of 0.4 dB/mm. The divergence from the calculation should come from the numerical dispersion of the FDTD method, and the effect of the off-axis propagation of the light in the actual waveguide.

Figure 13 shows a magnified view of the PBG characteristics of the samples with different designs. The minimum transmittance of sample B was as small as −27 dB. The length of the DBR part of the sample is only 1 mm, which is several orders smaller (or shorter) than the conventional band-rejection filters made with PLCs or fibers (FBGs).

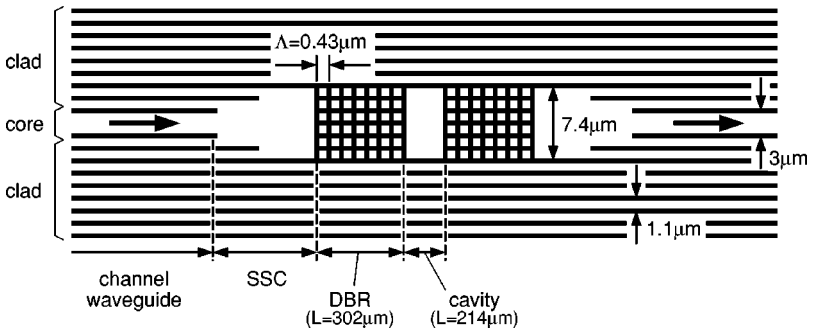

Fig. 14 Surface lattice geometry and designed structural parameters of an inline Fabry-Perot resonator. SSC stands for spot size converter.

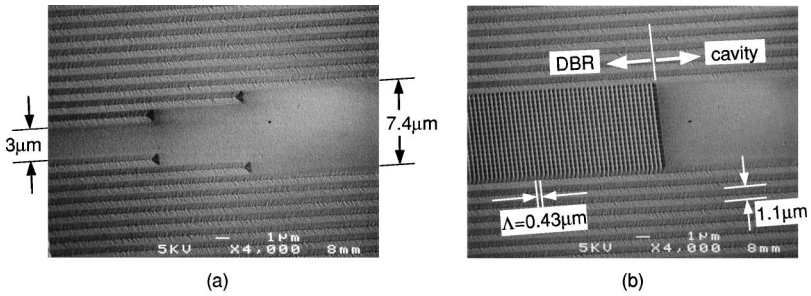

Fig. 15 SEM picture of the surface of a fabricated sample: (a) SSC part, and (b) near the interface between the DBR and SSC.

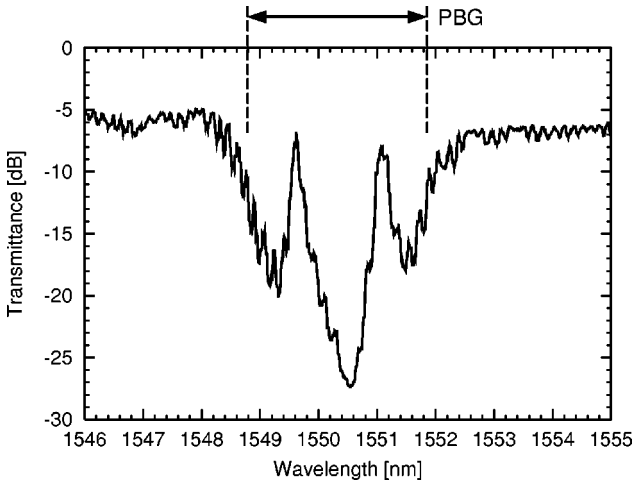

Fig. 16 Measured transmission spectrum of the resonator. Two resonance peaks with the FSR (free spectral range) of 1.45 nm are observed.

5 Functional Block 2: In-line Resonator

5.1 *Design and Fabrication*

By sandwiching a passband region with a pair of DBRs, we can form in-line Fabry-Perot resonators. An example of a surface lattice geometry for such resonators is shown in Fig. 14. The device consists of an input channel waveguide, a pair of DBRs with a cavity, and an output waveguide. The DBR consists of a 3-D periodic structure, whereas the channel waveguide and the cavity have a flat-multilayer core for enabling low-loss propagation. Spot-size converters (SSCs) are inserted between the channel and the DBR to efficiently use the PBG bandwidth of the DBR. Designed structural parameters are also shown in the figure. The cavity length of 214 μm is determined to make FSR=1.5 nm.

Figure 15 shows SEM pictures of the surface of the SSC part [Fig. 15(a)] and DBR/cavity interface [Fig. 15(b)], respectively. The domain boundaries of the heterostructure are perfectly defined.

5.2 *Characterization*

Figure 16 shows a measured transmission spectrum of a resonator. We obtained resonance wavelength=1549.6 nm,

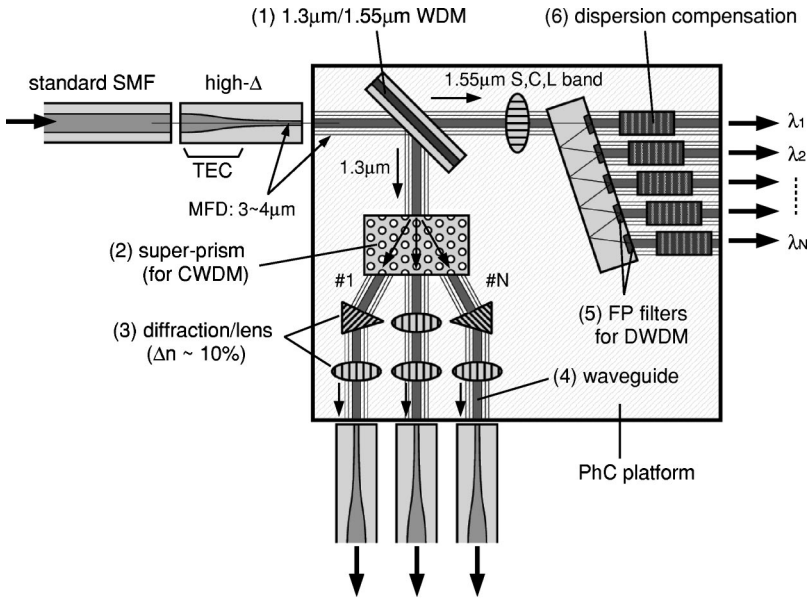

Fig. 17 Schematic illustration of an integrated optical chip consisting of heterostructured photonic crystals fabricated with the autocloning technology.

full-width at half matimum (FWHM)=0.13 nm, PBG width of ~3 nm, and the insertion loss at the resonance wavelength of 1.9 dB (compared to the passband loss). Loaded quality factor (Q_{loaded}), defined by $Q_{\text{loaded}}=\lambda_0/\text{FWHM}$, was 11,900. Such a sharp resonance characteristic largely attributes to the low-loss nature of the cavity region, and the scatter-free operation of the DBR. The performance of the resonator will be improved by, for example, a proper design of the DBR, or antireflection coatings on the waveguide ends.

6 Future Outlook

The concept of heterostructures, exemplified by waveguides, DBRs, and resonators, can be extended much farther. The beauty of autocloning is that lattices of the desired size can be stacked up at the desired positions with a common height (deposition rate) by a simple sputtering process. Just by corrugation patterns and sputtering, it is possible to produce almost arbitrary circuit functions such as delay compensators, in-plane lenses, superprisms, Bragg corner reflectors, and so forth, as shown in Fig. 17.

7 Conclusion

We explain the concept of photonic crystal chips made by heterostructured autocloned photonic crystals. We have confirmed that the pros 1 and 2 are achieved, and have established a means of overcoming cons 1, 2, and 3. The last problem to be solved is polarization dependence. The design of polarization-independent circuits may be achieved some day, but a more realistic scenario is to implement some functions that demonstrate the decisive superiority of photonic crystals that justifies the use of polarization diversity. The demonstration of such ''decisive superiority'' is the key issue for photonic crystal engineers.

Acknowledgments

This work was sponsored by the Special Correlation Funds for Promoting Science and Technology from the Ministry of Education, Culture, Sports, Science, and Technology, and supported by the Telecommunications Advancement Organization of Japan (TAO) and the Japan Science and Technology Agency(JST). Part of this work was carried out in the Laboratory for Electronic Intelligent Systems and the Venture Business Laboratory of Tohoku University.

References

1. H. Kosaka, T. Kawashima, A. Tomita, M. Notomi, T. Tamamura, T. Sato, and S. Kawakami, ''Superprism phenomenon in photonic crystals,'' *Phys. Rev. B* **58**, R10096–R10099 (1998).
2. S. Noda, A. Chutinan, and M. Imada, ''Trapping and emission of photons by a single defect in a photonic bandgap structure,'' *Nature (London)* **407**, 608–610 (2000).
3. E. Yablonovitch, ''Inhibited spontaneous emission in solid-state physics and electronics,'' *Phys. Rev. Lett.* **58**, 2059–2062 (1987).
4. J. D. Joannopoulos, P. R. Villeneuve, and S. Fan, ''Photonic crystals: putting a new twist on light,'' *Nature (London)* **386**, 143–149 (1997).
5. J. Arentoft, T. Sondergaard, M. Kristensen, A. Boltasseva, M. Thorhauge, and L. Frandsen, ''Low-loss silicon-on-insulator photonic crystal waveguides,'' *Electron. Lett.* **38**, 274–275 (2002).
6. A. Shinya and M. Notomi, ''Commensurate width-varied line-defect waveguides of SOI photonic crystal that can be bent,'' *Extended Abstracts (49th Spring Meet. 2002), Japan Soc. Appl. Phys. Related Soc.*, p. 1037 (2002).
7. N. Ikeda, H. Oda, Y. Sugimoto, T. Yang, K. Inoue, K. Ishida, and K. Asakawa, ''Bend efficiency improvement of defect waveguides for two-dimensional AlGaAs photonic crystal membranes,'' *Extended Abstracts (49th Spring Meet. 2002), Japan Soc. Appl. Phys. Related Soc.*, p. 1037 (2002).
8. A. Motegi and T. Baba, ''Calculation of transmittance at 60-degree-bend in photonic crystal line defect waveguide,'' *Extended Abstracts (49th Spring Meet. 2002), Japan Soc. Appl. Phys. Related Soc.*, p. 1038 (2002).
9. S. Kawakami, O. Hanaizumi, T. Sato, Y. Ohtera, T. Kawashima, N. Yasuda, Y. Takei, and K. Miura, ''Fabrication of 3D photonic crystals by autocloning and its applications,'' *Trans. Inst. Electron. Inf. Commun. Eng. C-I* **J81C-1**, 573–581 (1998).
10. K. Shiraishi, T. Yanagi, and S. Kawakami, ''Light-propagation characteristics in thermally-diffused expanded core fibers,'' *J. Lightwave Technol.* **11**, 1584–1591 (1993).
11. T. Sato, Y. Ohtera, N. Ishino, K. Miura, and S. Kawakami, ''In-plane light propagation in Ta2O5/SiO2 autocloned photonic crystals,'' *IEEE J. Quantum Electron.* **38**, 904–908 (2002).

Yasuo Ohtera received BE, ME, and PhD degrees in electronic engineering from Tohoku University, Sendai, Japan, in 1992, 1994, and 1997, respectively. In 1997, he joined the Research Institute of Electrical Communication, Tohoku University, as a research associate. He has been engaged in research on liquid crystal devices and analysis of thermally expanded core (TEC) fibers. His current research interest is the development of photonic crystal functional devices. Since June of 2001, he has been a research fellow of the New Industry Creation Hatchery Center (NICHe), Tohoku University. He is a member of the Institute of Electronics, Information, and Communication Engineers (IEICE) of Japan, and the Japan Society of Applied Physics.

Hiroyuki Ohkubo received BE and ME, degrees in the research laboratory of engineering materials from Tokyo Institute of Technology, Yokohama, Japan, in 1991 and 1993, respectively. He joined Hitachi Cable, Limited, Ibaraki-ken, Japan, in 1993, where he has been engaged in the research of optical waveguides. Since 2001, he has been a researcher of the New Industry Creation Hatchery Center (NICHe), Tohoku University. He has been engaged in research on photonic crystal waveguides. He is a member of the Institute of Electronics, Information, and Communication Engineers (IEICE) of Japan, and the Japan Society of Applied Physics.

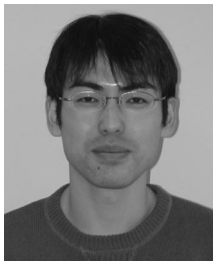

Kenta Miura received BS, MS, and PhD degrees in electrical communication engineering from Tohoku University, Sendai, Japan, in 1998, 2000, and 2003, respectively. Since April 2003, he has been a researcher of the Japan Science and Technology Agency. His research interest is in the development of photonic crystal devices. He is a member of the Institute of Electronics, Information, and Communication Engineers (IEICE) of Japan, and the Japan Society of Applied Physics (JSAP).

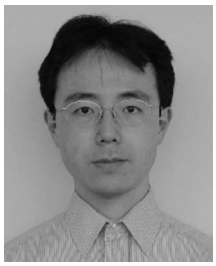

Takashi Sato received the BS, MS, and PhD degrees in electronic engineering from Tohoku University, Sendai, Japan, in 1989, 1991, and 1994, respectively. In 1994, he joined the Research Institute of Electrical Communication, Tohoku University, as a research associate. He has been engaged in research on thin-film optical components and integrated optical devices. His current research interest is in the development of photonic crystals and their application devices. Since June of 2001, he has been a research

fellow of the New Industry Creation Hatchery Center (NICHe), Tohoku University. He is a member of the Institute of Electronics, Information, and Communication Engineers (IEICE) of Japan, the Japan Society of Applied Physics, and the Optical Society of America.

Takayuki Kawashima received BE, ME, and PhD degrees in electronic engineering from Tohoku University, Sendai, Japan, in 1995, 1997, and 2000, respectively. From 1999 to 2001, he was a Research Fellow of the Japan Society for the Promotion of Science. Since 2001, he has been a Research Fellow of the New Industry Creation Hatchery Center (NICHe), Tohoku University. In 2002, he joined Photonic Lattice Incorporated. He was engaged in research on laminated polarization splitting devices. His current research interest is the development of the photonic crystal devices and the process for fabricating photonic crystals. He is a member of the Institute of Electronics, Information, and Communication Engineers (IEICE) of Japan, and the Japan Society of Applied Physics.

Shojiro Kawakami received the BS degree in 1960, the MS degree in 1962, and the PhD degree in 1965, all from the University of Tokyo. In 1965, he joined the Research Institute of Electrical Communication, Tohoku University, Sendai, Japan, and in 1979 he was promoted to professor. Since 2000, he has been with New Industry Creation Hatchery Center(NICHe), Tohoku University. In the 1960s and 1970s, his main interest was in optical fiber theory. His main work in fiber optics is the discovery of the group-velocity equalization effect of graded index fibers (1967) and the invention of W fibers (1974). In the 1980s and 1990s, he was interested in microoptic components. His main works in this period include optical isolators, laminated polarizers (LAMIPOLs), thermally diffused expanded core (TEC) fibers, etc. Since 1997 he has been engaged in the research and development of photonic crystals. In 2002, he established Photonic Lattice Incorporated, a start-up company for producing autocloned photonic crystals.